

## Short communication

## Fabrication of highly porous LSM/CGO cell stacks for electrochemical flue gas purification

Kjeld Andersen, Frantz Bræstrup, Kent Kammer Hansen\*

*Department of Energy Conversion and Storage, Technical University of Denmark, DTU, Frederiksborgvej 399, DK-4000 Roskilde, Denmark*

Received 3 July 2012; received in revised form 24 July 2012; accepted 25 July 2012

Available online 7 August 2012

**Abstract**

In this study porous cell stacks for electrochemical flue gas purification were fabricated using tape casting and lamination followed by sintering. Two different mixtures of pore formers were used; either a mixture of two types of graphite or a mixture of graphite with polymethyl methacrylate micro-particles. It was shown that the porous cell stacks fabricated with polymethyl methacrylate had a higher porosity but a similar back pressure compared to the porous cell stacks fabricated with only graphite as a pore former. This was due to a high back pressure of the electrolyte layer. The porous cell stacks fabricated with polymethyl methacrylate as a pore former seem to be well suited for i.e. capture of soot particles. Furthermore, the back pressure of the electrode layer was significantly reduced when using polymethyl methacrylate pore formers. However, a better interconnectivity of the pores formed by the polymethyl methacrylate pore former, especially in the electrolyte layer, is needed, in order to lower the back pressure of the porous cell stack.

© 2012 Elsevier Ltd and Techna Group S.r.l. All rights reserved.

**Keywords:** A. Tape casting; LSM; CGO; Lamination

**1. Introduction**

Pollutants emitted from the combustion of fossil fuels are an increasing problem, especially in urban areas. The main pollutants emitted are particulate matter, hydrocarbons, CO and NO<sub>x</sub> [1]. Whereas the three-way catalytic converter can remove hydrocarbons, CO and NO<sub>x</sub> from the exhaust from petrol fired Otto engines, it is not able to remove NO<sub>x</sub> from the exhaust emitted from Diesel fired engines, due to the excess of oxygen in the exhaust [2,3]. Other methods for removal of NO<sub>x</sub> from the exhaust from Diesel fired engines therefore have to be developed. The concept used at present is the selective catalytic reduction (SCR) of NO<sub>x</sub>. Here a reducing agent is added to the exhaust stream, and brought to react with the NO<sub>x</sub> on a suitable catalyst [4]. The main problems with this technique are the need of storage of the reducing agent on board the vehicle and a possible slip of the reducing agent. Another approach is to use an all solid state electrochemical cell, as suggested by Pancharatnam et al. [5].

Electrochemical gas cleaning is based on selective membrane processes, where an electrical current (electrons) is used as a reagent. Such processes can be optimized to remove pollutants from exhaust gases in a more sustainable and economically advantageous way than the known traditional catalytic exhaust gas treatment methods. An electrochemical membrane consists of an electrolyte that separates a set of porous electrodes, just like in a fuel cell. The electrolyte can conduct ions, but not electrons. The electrodes act as catalysts for the electrochemical reactions (see Fig. 1) [6]. This type of system allows a portfolio of selective reactions to occur at the electrodes.

In earlier work it was shown that porous cell stacks for electrochemical flue gas purification can be made by tape casting, lamination and sintering [7]. However, the porosity of the porous cell stacks is too low, leading to high a back pressure. In this work the fabrication of highly porous cell stacks for electrochemical flue gas purification is described. In this study some of the graphite was replaced with polymethyl methacrylate (PMMA) micro-particles in order to increase the porosity of the porous cell stacks. It is shown that highly porous cell stacks can be fabricated with a proper choice of pore former. The porous

\*Corresponding author. Tel.: +45 4677 5835.

E-mail address: [kkha@dtu.dk](mailto:kkha@dtu.dk) (K. Kammer Hansen).

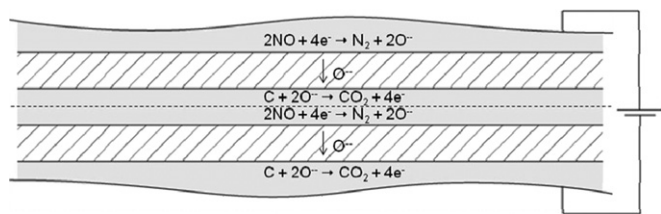


Fig. 1. The principle of operation for an electrochemical filter unit for removal of  $\text{NO}_x$ . When the unit is polarized  $\text{NO}_x$  is reduced at the cathode, and the soot is oxidized at the anode.

cell stacks consists of a LSM–CGO ( $(\text{La}_{0.85}\text{Sr}_{0.15})_{0.9}\text{MnO}_3\text{--Ce}_{0.9}\text{Gd}_{0.1}\text{O}_{1.95}$ ) composite electrode and a CGO electrolyte. The porous cell stacks were characterized by scanning electron microscopy and flow measurements.

## 2. Experimental

### 2.1. Preparation of slurries

The powders used in the present study were LSM from Haldor Topsøe A/S, Denmark and CGO from Rhodia, France. As pore formers graphite from Alfa Aesar and PMMA micro-particles from Esprix Technologies (MR10G) were used.

The fabrication of slurries with PMMA is described below. A similar procedure was used for fabrication of the slurries with only graphite added as a pore former.

**Electrode:** LSM powders calcined at 800 °C and 1200 °C were mixed in the ratio 1:1 and suspended in an azeotropic mixture of methylethylketone and ethanol (MEKET) with polyvinylpyrrolidone (PVP) or polyethyleneimine (PEI) as dispersant. After ball milling the suspension for 2 days, CGO (35 wt% of powder) and PVP were added and the suspension was milled for additional 24 h. Then 11.2 wt% PMMA micro-particles and 4.8 wt% graphite (2.6  $\mu\text{m}$ ) were added and the suspension was milled for 5 h. Finally a mixture of binder, plasticizer and a release agent was added and the suspension was milled overnight. The compositions of the electrode slurries are given in Table 1.

**Electrolyte:** CGO, MEKET and PEI were mixed and the suspension was milled for additional 24 h. Then 11.2 wt% PMMA micro-particles and 4.8 wt% graphite (2.6  $\mu\text{m}$ ) were added and the suspension was milled for 5 h. Finally a mixture of binder, plasticizer and a release agent was added and the suspension was milled overnight. The compositions of the electrolyte slurries are likewise given in Table 1.

### 2.2. Characterization of slurries

The particle size distribution (PSD) was measured after each step using a laser diffraction particle size analyzer (LS13320, Beckman Coulter, USA). The viscosity of the suspension was measured before tape casting using a Haake RheoStress 600 rheometer (Thermo-scientific, USA) with

Table 1  
Slurry composition. All values are in grams.

	PMMA tapes		Graphite tapes	
	Electrode	Electrolyte	Electrode	Electrolyte
LSM 1200 °C	107		107	
LSM 800 °C	107		107	
PVP (33%) in MEKET	13		13	
MEKET	20		20	
CGO	115	126	115	126
PVP (33%) in MEKET	7		7	
PEI		5		5
MEKET	67	88	67	88
Graphite (flake DD=10 $\mu\text{m}$ )			46	17
PMMA	46	17		
Graphite (round DD=2.6 $\mu\text{m}$ )		10		10
PVP (33%) in MEKET		4		
Binder	268	104	275	126

Table 2  
Viscosity and particle size of the slurries used in this study.

	PMMA		Graphite	
	Electrode	Electrolyte	Electrode	Electrolyte
Viscosity mPas at shear rate 4 s <sup>-1</sup>	1900	1173	1633	1200
Particle size, D, 50 $\mu\text{m}$	1.64	0.75	1.30	0.65

parallel plate configuration and 0.1 mm separation between the plates. The suspensions were adjusted to the desired viscosity prior to tape casting Table 2.

Thermogravimetry was measured using a Netzch STA 409 CD thermo balance.

### 2.3. Tape casting of slurries

The electrode suspension was tape casted, using a doctor blade adjusted to 0.25 mm, at a casting speed of 20 cm/min. The electrolyte suspension was tape casted, using a doctor blade adjusted to 0.20 mm, at a casting speed of 20 cm/min.

### 2.4. Lamination and sintering

When the tapes were dry, the tapes were laminated together in an 11-layers unit with alternating layers of electrode and electrolyte (6 electrodes and 5 electrolytes) as described by Larsen and Brodersen [8]. The tapes were laminated at a temperature of 130 °C. After lamination the samples were sintered at 1250 °C for 4 h.

The shrinkage of the samples during sintering was characterized by measuring the change in dimensions upon sintering. The micro-structure of the sintered samples was examined in Hitachi tabletop microscope (TM1000) and the porosities were characterized by mercury porosimetry

(AutoPore IV, Micromeritics, USA). The back pressure was measured using a special designed setup.

### 3. Results and discussion

#### 3.1. Lamination and sintering

The lamination occurred without any problems, and the tapes were well adhered in the green state. At first the sintering, of the laminated green tapes, was performed as described by He et al. [7]; see Table 3, program 1. This sintering profile resulted in perfect flat crack free cells when using only graphite as a pore former. However, when PMMA was used as a pore former the cells cracked during sintering. This is probably due to the cells getting adhered to the substrate during sintering. The sintering profile was therefore altered slightly; see Table 3, program 2.

It was concluded that the cracking of the cells was due to melting of the PMMA and binder during the initial stages of heating. The de-binding heating profile was therefore changed, with a heating rate of 6 °C/h up to 220 °C with holding the temperature constant at 80 °C and 220 °C for 10 h. 80 °C was chosen as it is just above the boiling point of MEKET, and 220 °C was chosen from the DTG curve in Fig. 2, which shifts due to the burning of the binder. So the new program allows for the removal of MEKET and binder, before the binder softening, thereby preventing the binder in the cells to adhere to the substrate during the initial states of the sintering. The new program did avoid

Table 3

The sintering profiles used in this study. Maximum temperature is 1250 °C for 4 h.  $T$  is the temperature in °C,  $R$  is ramp in °C/h and  $H$  is holding time in hours.

Program no.	Heating	Sintering	Cooling
1	$T=400$ , $R=20$ , $H=2$ $T=600$ , $R=20$ , $H=4$ $T=800$ , $R=20$ , $H=2$	$T=1250$ $R=60$ $H=4$	$T=25$ $R=60$
2	$T=80$ , $R=6$ , $H=10$ $T=220$ , $R=6$ , $H=10$ $T=400$ , $R=20$ , $H=6$ $T=600$ , $R=20$ , $H=10$	$T=1250$ $R=120$ $H=4$	$T=25$ $R=120$

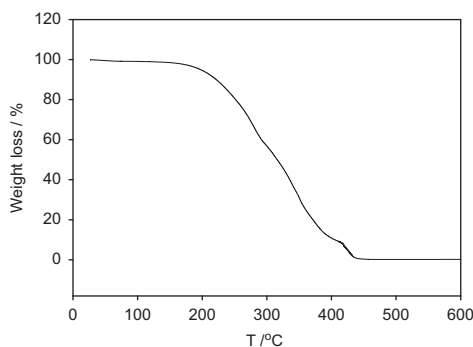


Fig. 2. Weight loss of the binder solution in percent. The burn off of the binder is initiated at around 200 °C.

the adhering of the cells to the substrate and resulted in perfectly flat crack free cells.

#### 3.2. Results of sintering

The shrinkage of the cells with only graphite as a pore former is 27.4% and the porosity is 31%. The shrinkage of the cells with the PMMA pore former on the other hand is 27.9% and the porosity is 41.9%. This shows that highly porous cell stacks can be fabricated by replacing some of the graphite with PMMA Table 4.

#### 3.3. SEM

Micro-graphs of the sintered porous cell stacks are shown in Figs. 3–6. The figures show an 11-layer structure in a symmetric setup. The darker areas are the electrode, LSM/CGO, and the lighter areas are the CGO electrolyte. The 11-layers are well adhered, giving a good contact between the 2. In Figs. 3 and 4 a porous cell stack fabricated using only graphite as a pore former is shown. It is seen that the structure is porous, with many pores of different dimensions. The larger pores are seen to be aligned in the tape cast direction. This is not needed as it is perpendicular to the flow direction, leading to a high back-pressure. In Figs. 5 and 6 a porous cell stack fabricated using PMMA as a pore former is shown. It is seen that the structure contains many

Table 4

The porosity and shrinkage in percent. The porosity of the cells fabricated with PMMA is significant higher for the cells where only graphite was used as a pore former.

Type	Porosity (%)	Shrinkage (%)
PMMA	41.9	27.9
Only graphite	31.0	27.4

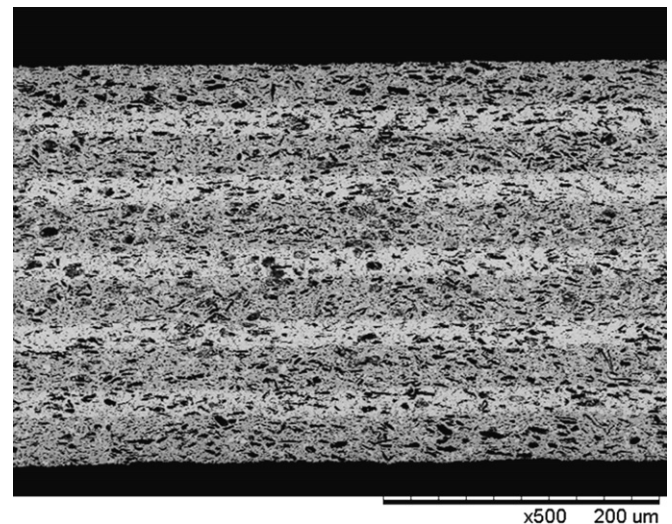


Fig. 3. The 11-layers porous cell stack, with only as pore former. The darker areas are electrode and the lighter areas are electrolyte. The structure is highly porous.



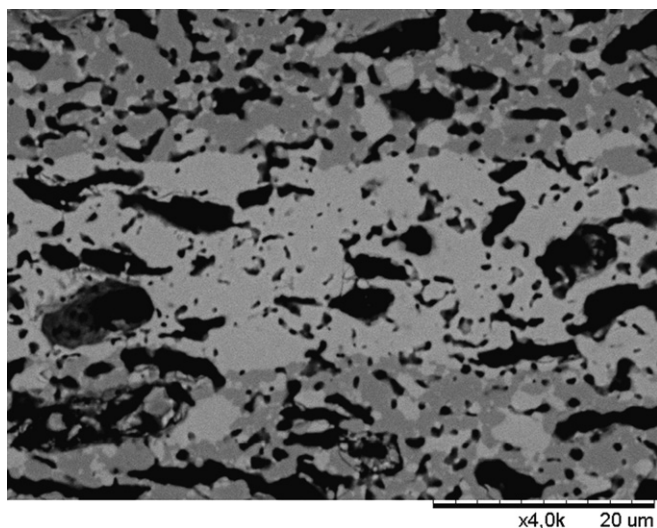


Fig. 4. A section of the 11-layered porous cell stack that only contains graphite as pore former. The darker areas are electrode and the lighter areas are electrolyte.

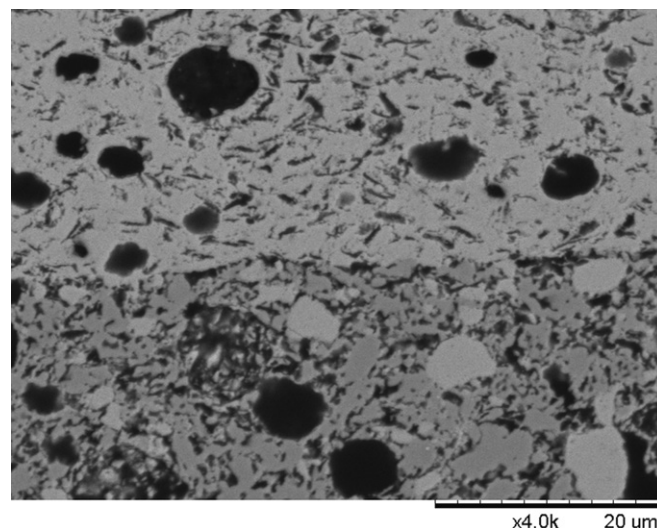


Fig. 6. A section of the porous cell stack, with spherical PMMA particles has been used as the pore former. The darker areas are electrode and the lighter areas are electrolyte. The large pores are seen to be isolated in the structure in the electrolyte layers.

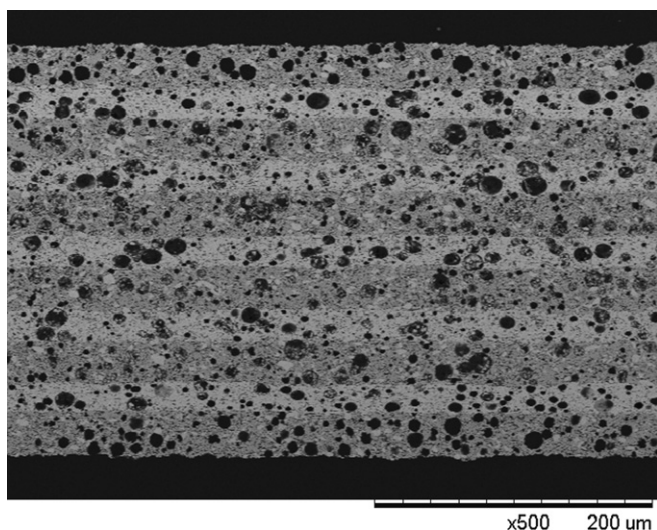


Fig. 5. The 11-layers porous cell stack, with PMMA/graphite as pore former. The darker areas are electrode and the lighter areas are electrolyte. Many large pores are present in the structure.

large pores, which are almost circular in shape. The pores are well distributed in both the electrode and electrolyte layers. The largest pores are around 10  $\mu\text{m}$  in diameter. The large pores are seen to be isolated in the structure in the electrolyte layers. Many smaller pores are also observed in the structure, especially in the electrode layers. The micro-structure of the electrodes layers could be well suited for caption of soot particles. Some agglomeration of the CGO particles is observed and this will be addressed in an upcoming work.

### 3.4. Back pressure

The flow through the cells as a function of back pressure is shown in Tables 5a and 5b. It is seen that the back

Table 5a

Flow as a function of back pressure. The flow is given in  $\text{mL/min. cm}^2$ , the back pressure in mbar. The back pressures of the two types of cells are similar.

PMMA		Graphite	
Flow	Pressure	Flow	Pressure
0	0	0	0
3.18	31	3.18	32
3.98	34	3.98	34
4.77	41	4.77	40
5.57	48	5.57	47
6.37	54	6.37	53

Table 5b

The back pressure as a function of flow, in the individual layers. The flow is given in  $\text{mL/min. cm}^2$ , the back pressure in mbar. The electrode layers with LSM and PMMA have the lowest backpressure.

Flow	Pressure			
	CGO-PMMA	LSM-PMMA	CGO-C	LSM-C
0	0	0	0	0
3.18	19	7	12	15
3.98	23	8	15	16
4.77	26	9	17	20
5.57	31	10	21	23
6.37	34	11	24	27
Thickness ( $\mu\text{m}$ )	250	200	200	260

pressure for the cell fabricated with PMMA is almost the same as for the cell fabricated with only graphite at a given flow. However, looking at the back pressure for the individual layers, it is seen that the back pressure is much lower in the electrode layer, where PMMA is used as a

pore former. Furthermore, the back pressure of electrolyte layer fabricated with the PMMA pore is higher than that for the other layers. This indicated that the pores formed by the PMMA, in the electrolyte layers, are closed porosities, and that the large pores are not interconnected. Further work will aim at creating a better interconnectivity of the large pores, in the electrolyte layers.

#### 4. Conclusion

It has been shown that highly porous cell stacks for electrochemical flue gas purification can be made by a proper choice of pore former. The porosity could be increased but the back pressure was kept constant if part of a graphite pore former was replaced with PMMA micro-spheres. The high back pressure of the PMMA based cell was due to the electrolyte layer. The electrode layer of the PMMA based cells had a much lower back pressure than the other layers studied in this work. The structure of the PMMA based cells seems well suited for caption of i.e. soot particles. This is a step forward in the fabrication of a full ceramic highly porous cell stack for electrochemical flue gas purification.

#### Acknowledgments

Colleagues at the Department are thanked for their help with preparation of the samples. The strategic research council of Denmark is thanked for financial support (09-065186).

#### References

- [1] G.C. Koltsakis, A.M. Stamatelos, Catalytic automotive exhaust after treatment, *Progress in Energy and Combustion Science* 23 (1997) 1.
- [2] K.C. Taylor, in: M. Kong, L. Huang (Eds.), *Frontiers of Materials Research/Electronic and Optical Materials*, Elsevier, Amsterdam, 1991, pp. 46–56.
- [3] J. Kaspar, P. Fornasiero, N. Hickey, Automotive catalytic converters: current status and some perspectives, *Catalysis Today* 77 (2003) 419.
- [4] H. Bosch, F. Janssen, Preface, *Catalysis Today* 2 (1988).
- [5] S. Pancharatnam, R.A. Huggins, D.M. Mason, Catalytic decomposition of nitric oxide on zirconia by electrolytic removal of oxygen, *Journal of the Electrochemical Society* 122 (1975) 869.
- [6] K.B. Andersen, F.B. Nygaard, Z. He, M. Menon, K.K. Hansen, Optimizing the performance of porous electrochemical cells for flue gas purification using the DOE method, *Ceramics International* 37 (2011) 903.
- [7] Z. He, K.B. Andersen, L. Keel, F.B. Nygaard, M. Menon, K.K. Hansen, Processing and characterization of porous electrochemical cells for flue gas purification, *Ionics* 15 (2009) 427.
- [8] P.H. Larsen, K. Brodersen, Improved method for the manufacture of reversible solid oxide cells, Patent no. (2008) US2008124602-A1; JP2008130568-A; EP1930974-A1; CN101242003-A; CA2611362-A1; KR2008047282-A; KR966845-B.